Chemical Science

Accepted Manuscript

This article can be cited before page numbers have been issued, to do this please use: Q. Ye, L. Ponomareva, Y. Cao, Y. Liu, Z. Cui, S. Van Lanen, S. R. Voss, Q. She, Y. Zhang and J. S. Thorson, *Chem. Sci.*, 2019, DOI: 10.1039/C9SC02289A.

ROYAL SOCIETY OF CHEMISTRY

rsc.li/chemical-science

View Article Online
DOI: 10.1039/C9SC02289A

ARTICLE

Total synthesis of griseusins and elucidation of the griseusin mechanism of action

Received 00th January 20xx,
Accepted 00th January 20xx

DOI: 10.1039/x0xx00000x

Yinan Zhang,[a,b,c,†] Qing Ye,[d,†] Larissa V. Ponomareva,[b,c] Yanan Cao,[d] Yang Liu,[b,c] Zheng Cui,[c] Steven G. Van Lanen,[c] S. Randal Voss,[e] Qing-Bai She,*[,d] Jon S. Thorson*[,b,c]

A divergent modular strategy for the enantioselective total synthesis of 12 naturally-occurring griseusin type pyranonaphthoquinones and 8 structurally-similar analogues is described. Key synthetic highlights include Cu-catalyzed enantioselective boration-hydroxylation and hydroxyl-directed C-H olefination to afford the central pharmacophore followed by epoxidation-cyclization and maturation via diastereoselective reduction and regioselective acetylation. Structural revision of griseusin D and absolute structural assignment of 2a,8a-epoxy-*epi*-4'-deacetyl griseusin B are also reported. Subsequent mechanistic studies establish, for the first time, griseusins as potent inhibitors of peroxiredoxin 1 (Prx1) and glutaredoxin 3 (Grx3). Biological evaluation, including comparative cancer cell line cytotoxicity and axolotl embryo tail inhibition studies, highlights the potential of griseusins as potent molecular probes and/or early stage leads in cancer and regenerative biology.

Introduction

Pyranonaphthoquinone (PNQ) natural products represent an array of structurally and functionally diverse bacterial secondary metabolites.[1] Despite extensive advances in PNQ synthetic methodology,[2-3] the commercial application of PNQs as feedstock additives and the demonstrated anticoccidial and antimalarial efficacy of PNQs,[4] the mechanism of action for PNQs remained unresolved. Enabled by our efficient divergent strategy for the synthesis of frenolicin B (**FB**, a prototypical PNQ-based natural product; Figure 1),[2f] systematic SAR and mechanistic studies revealed **FB** as the most potent and selective peroxiredoxin 1 (Prx1) and glutaredoxin 3 (Grx3) inhibitors reported to date.[5] These studies demonstrated Prx1/Grx3 inhibition by **FB** led to increased intracellular ROS, the consequence of which was inhibition of mTORC1-mediated 4E-BP1 phosphorylation, apoptosis induction and tumor suppression. Whether this fundamental mechanism of action is unique to **FB** or more broadly attributed to the other diverse PNQ family members remains to be determined.

First reported in 1976, the griseusin-based PNQ metabolites are structurally distinguished by their fused spiro-ring C/E system (Figure 1) in lieu of the FB C1-alkyl side chain of FB.[6] Griseusin members are further differentiated via ring D forms (open or closed), relative stereochemistry, oxidation, glycosylation, and/or O- or C-acetylation. Like their frenolicin counterparts, many of the griseusins display potent cancer cell line cytotoxicity. Representative griseusins have also been reported as COMPARE negative (indicating a novel mechanism of activity)[6g] and potentially synergistic with tumor necrosis

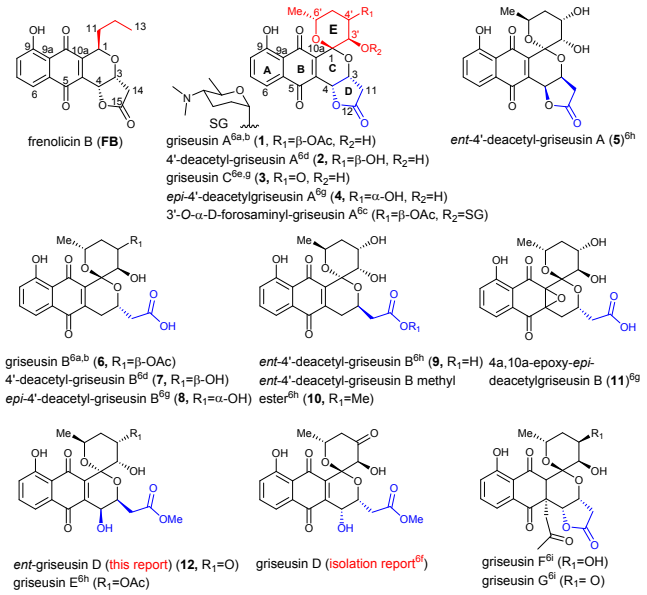

Figure 1. Naturally-occurring frenolicin prototype (FB) and griseusins.

[a.] *Jiangsu Key Laboratory for Functional Substances of Chinese Medicine, School of Pharmacy, Nanjing University of Chinese Medicine, Nanjing, Jiangsu, 210023, China.*
[b.] *Center for Pharmaceutical Research and Innovation*
[c.] *College of Pharmacy, University of Kentucky, Lexington, KY 40536, USA. E-mail: jsthorson@uky.edu*
[d.] *Markey Cancer Center and Department of Pharmacology and Nutritional Sciences, College of Medicine, University of Kentucky, Lexington, KY 40536, USA. E-mail: qing-bshe@uky.edu*
[e.] *Department of Neuroscience, Spinal Cord and Brain Injury Research Center, Ambystoma Genetic Stock Center, University of Kentucky, Lexington, KY 40536, USA*
† These authors contributed equally.
Electronic Supplementary Information (ESI) available: [details of any supplementary information available should be included here]. See DOI: 10.1039/x0xx00000x

View Article Online DOI: 10.1039/C9SC02284A

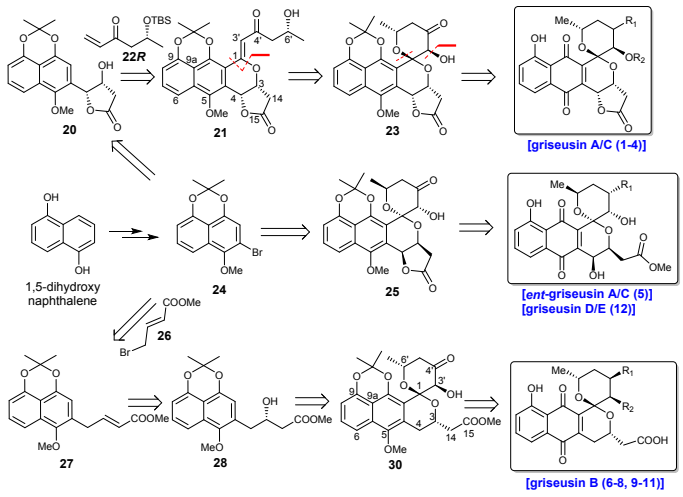

Scheme 1. Retrosynthetic analysis for griseusin subclasses A-E

factor-related apoptosis-inducing ligand (TRAIL) in TRAIL-resistant gastric adenocarcinoma cell lines.[6h] Yet, the molecular target and mechanism of action for griseusin remains unknown.

Enabled by our recently reported synthetic approach to griseusin A (**1**), 4′-deacetyl-griseusin A (**2**), and griseusin C (**3**),[3m] herein we report the further development and implementation of the first concise divergent synthetic approach to a broad set of griseusin A-E analogs (twelve naturally-occurring griseusins and eight additional synthetic analogues). Methodological highlights include mechanistic investigation of C-H olefination *en route* to the griseusin C-ring, enantioselective Cu-catalyzed boration-hydroxylation to afford open D-ring griseusin B members and a series of stereoselective and regioselective transformations for E-ring diversification. This enabling chemistry also facilitated revision of the previous reported griseusin D structure, assignment of stereocenters in 4a,10a-epoxy-*epi*-4′-deacetyl griseusin B and the broadest griseusin comparative cancer cell line cytotoxicity SAR analysis to date. Subsequent biochemical and cell-based studies revealed representative griseusins to inhibit Prx1/Grx3 and 4E-BP1 phosphorylation in manner similar to **FB** and to inhibit tail regeneration in our recently developed axolotl tail regeneration assay.[7] Given the notable demonstrated in vivo efficacy of optimized FB analogs,[5] the current study considerably expands the range PNQ pharmacophores available for further optimization of Prx1/Grx3 selectivity and/or ADMET.

Results and discussion

2.1 Retrosynthetic analysis and rationale.

Scheme 1 highlights a conceptual overview of the envisioned synthetic route to griseusin-type PNQs. C1 epimerization within the context of spiropyran construction and/or subsequent scaffold maturation presents a primary hurdle to griseusin total synthesis. We postulated that diastereoselective C1-C3′ epoxidation and subsequent C6′-OH intramolecular cyclization could provide the key spiro-pyrano core **23**, the C1 stereocenter of which should be stable to late-stage deprotection of the acetonide.[8] For this approach, the critical **21** C1-C3′-enone would derive from simple convergent C-H olefination using **20** and **22R**, the latter of which would result from Sharpless asymmetric dihydroxylation[9] of the Heck-coupled product of methyl 3-butenoate and bromine **24**. Following the same strategy, *ent*-griseusin C (and the griseusin D/E subclass) may derive from enantiomer **25** and AD-mix-α. For the griseusin B series, alcohol **28** would stem from copper-catalyzed enantioselective boration-hydroxylation[10] of **27**, accessible via a palladium coupling between bromine **26** and a **24**-derived boronic acid. Final maturation/tailoring reactions would also leverage the C4′ ketone of precursors **23**, **24** and **30** where applicable.

2.2 Synthesis of key griseusin A/C precursors.

A range of conditions were explored for reduction of the **32**[3m] C4′ ketone, the primary goal of which was to establish a general reductive method with bilateral C4′ diastereoselectivity (Table S1 and Scheme 2). Among the common borohydride reagents (Table S1, entries 1-2), K selectride provided the desired β-alcohol **33** exclusively in a 94% isolated yield compared to the observed 4:1 diastereoselectivity with $NaBH_4$ (Table S1, entry 1). Non-ionic boranes favored formation of the desired α-alcohol **34** with the borane 2-picoline complex in the presence of HCl providing the best diastereoselectivity (Table S1, entries 3-11).[11] Solvent optimization (Table S1, entries 12-15) revealed that reactions in ether provided the desired α-alcohol in 75% isolated yield with 1:10 diastereoselectivity (Table S1, entry 15). Putative mechanistic rationale for diastereoselectivity in this reaction is based on sterics (favoring hydride attack from the *si*-face to give (*R*)-alcohol **33**) or partial spiroketal oxygen-borane coordination (favoring hydride attack from the *re*-face to give (*S*)-alcohol **34**).

A similar optimization strategy was pursued for reduction of the **23** C4′-carbonyl to set the stage for the synthesis of C3′/4′-diols (Table S2). Electrophilic reducing agents, such as sodium borohydride and lithium borohydride, provided the desired C4' *cis*-diol **35** in high yield and *si*-facial selectivity (Scheme 2). In contrast, this study failed to identify suitable reductive conditions to furnish the corresponding desired *trans*-diol **36**, potentially due to C3′-OH infringement on the putative spiroketal oxygen-borane coordination required for stereoselective hydride delivery. As an alternative, benzyl protective intermediate **37** led to the *re*-face C4′-carbonyl stereospecific reduction reminiscent to that for (*S*)-alcohol **34** (Table S3). The corresponding **23** protection/reduction/deprotection protocol afforded the desired *trans*-diol **36** in a 54% cumulative yield for three steps (Scheme 2).

With diol **35** in hand, we next evaluated regioselective O-acetylation (Table S4). Initial attempts to obtain the desired products **39-41** via mild transesterification[12] were hampered by poor diol reactivity (Table S4, entries 1-2). Use of acetic anhydride and base optimization led to the desired products in variable yields (Table S4, entries 3-8). Specifically, use of a sterically-hindered base favored the desired C4′-acetylation (Table S4, entry 6) while relatively weak base gave exclusive C3′-acetylation (Table S4, entry 7). Reduction of the amount of

base and acetic anhydride further improved yield (Table S4, entry 8) while the use of a nucleophilic strong base favored peracetylated product **41** (Table S4, entry 9).

2.3 Synthesis of key griseusin B precursors.

The route to griseusin B analogues began with the synthesis of **42** following standard methodology for lithium-bromine exchange-mediated boronic acid generation (Scheme 3). Palladium-catalyzed Suzuki coupling[13] of **42** with bromobutenoate (**26**) gave **27**. With α,β-unsaturated ester **27** in hand, we investigated a range of β-borylation conditions for enantioselective β-conjugate addition (Table S5). This small study revealed chiral diphosphine ligand[10] as advantageous over bisoxazoline and *N*-heterocyclic carbene catalysts,[14] enabling quantitative yield with 90% enantioselectivity on gram scale.

Subsequent installation of **29*R*** (to access the desired 1-methylene isochroman **43**, Scheme 4) began with our C-H activation C1 olefination conditions for **20**.[3m] While these initial conditions (Table S6, entry 1) were sub-optimal in this case, subsequent modification of reaction solvent (Table S6, entries 2-4) and catalyst/oxidant loading (Table S6, entries 4-8) gave the desired 1-methylene isochroman **43** in 66% on gram scale (Table S6, entry 9). The lower observed abundance of side product **52** in these C1 olefination studies implicated the flexible secondary alcohol of **28** (compared to the corresponding rigid secondary alcohol of **20**) as advantageous. Access to **53** also facilitated further mechanistic investigation of this C-H olefination event (Scheme 4). Specifically, intermediate **53** results from initial hydroxyl-assisted C-H insertion of Pd (II) followed by β-elimination and subsequently enters the second round of Pd-catalyzed intra-molecular oxidative cyclization (eq 1). In contrast, side product **52** cannot undergo β-elimination (eq 3) and therefore irreversibly consumes **53** as a major competing reaction (eq 2). The bifurcation between the desired product (*e.g.*, 1-methylene isochroman **43**) and undesired shunt products (*e.g.*, **52**) is presumably dictated by a propensity for palladium

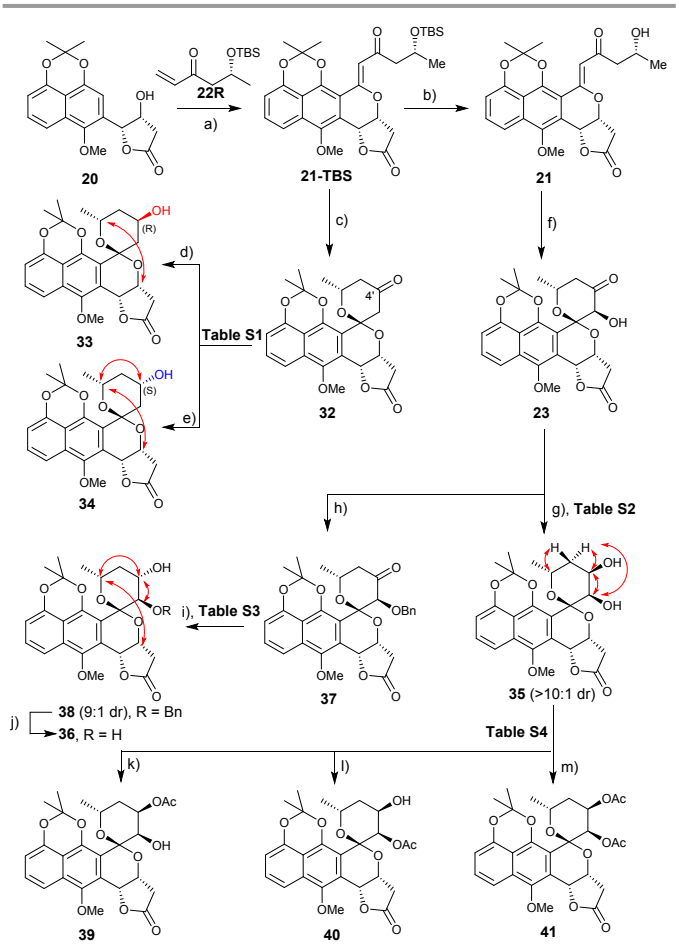

Scheme 2. Synthesis of griseusin A/C-type analogues. Key NOE crosspeaks are highlighted (red arrows). Reagents and conditions: (a) $Pd(OAc)_2$ (20 mol%), Li_2CO_3, Ag_2CO_3 (4 eq), DCE, 80 °C, 16 h, 40%; (b) HF·pyridine (10 eq), TEA (2 eq), dioxane, rt, 16 h, 85%; (c) HF·pyridine (10 eq), CH_3CN, rt, 16 h, 91%; (d) K-selectride, THF, -78 °C, 2 h, 94%; (e) BH_3·2-picoline, HCl, Et_2O, 16 h, 75%; (f) DMDO, TfOH, DCM, -78 °C-0 °C, >10:1 dr, 80%; (g) $LiBH_4$ (2 eq), THF, -78 °C, 0.5 h, 85%, β:α >10:1; (h) KOtBu (2 eq), BnBr (2 eq), THF, 0 °C-rt, 16 h, 77%; (i) BH_3·Me_3N (2 eq), TFA (3.0 eq), ether, rt, 36 h, 74%, α:β = 9:1; (j) Pd/C, H_2, MeOH, rt, 4 h, 95%; (k) Ac_2O (10 eq), dichylohexymethyl amine (10 eq), DCM, rt, 40 h, 70%; (l) Ac_2O (5 eq), pyridine (5 eq), DCM, rt, 16 h, 88%; (m) Ac_2O (10 eq), DABCO (10 eq), DCM, rt, 16 h, 93%.

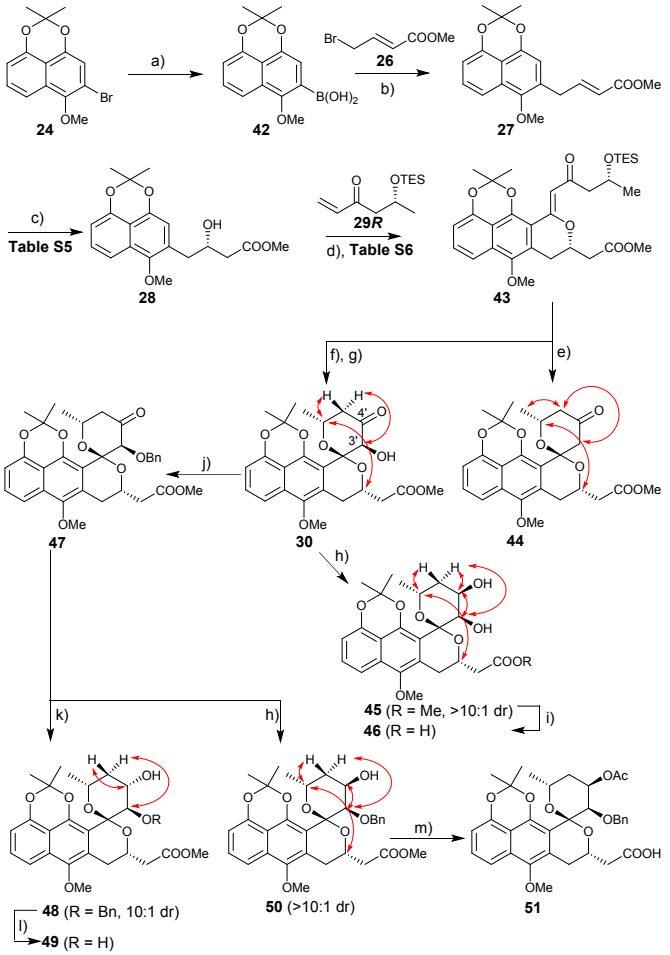

Scheme 3. Synthesis of griseusin B-type analogues. Key NOE crosspeaks are highlighted (red arrows). Reagents and conditions: (a) nBuLi, $B(OiPr)_3$, THF, -78 °C, 2 h, 80%; (b) **26**, $Pd(OAc)_2$, KF, dioxane, rt, 2 h, 74%; (c) 1.5 mol% CuCl, 3 mol% *S*-R_p-josiphos, 2.5 mol% NaOtBu, $Bpin_2$, THF, 0 °C-rt, 16 h; then $NaBO_3$, H_2O, rt, 2h, 91%, 90% ee; (d) **29**, 40 mol% $Pd(OAc)_2$, Ag_2CO_3 (2eq), Li_2CO_3, $CHCl_3$, 80 °C, 16 h, 63%; (e) HF·pyridine, CH_3CN, rt, 12h, 81%; f) HF·pyridine, TEA, dioxane, rt, 1h, 88%; g) DMDO, 50 mol% TfOH, DCM, -78 °C-(-20)°C, 2h, 93%; h) $LiBH_4$ (2 eq), THF, -78 °C, 0.5 h, 86%, β:α >10:1; i) 1N LiOH, MeOH, rt, 1h, 95%; j) BnBr, Ag_2O, NMP, rt, 36 h, 76%; (k) BH_3·Me_3N (2 eq), TFA (3.0 eq), ether, rt, 36 h, 77%, α:β = 10:1; (l) Pd/C, H_2, MeOH, rt, 4 h, 93%; m) 1N LiOH, MeOH, rt, 1h; Ac_2O, DABCO, DCM, rt, 40 h; 65% for two steps.

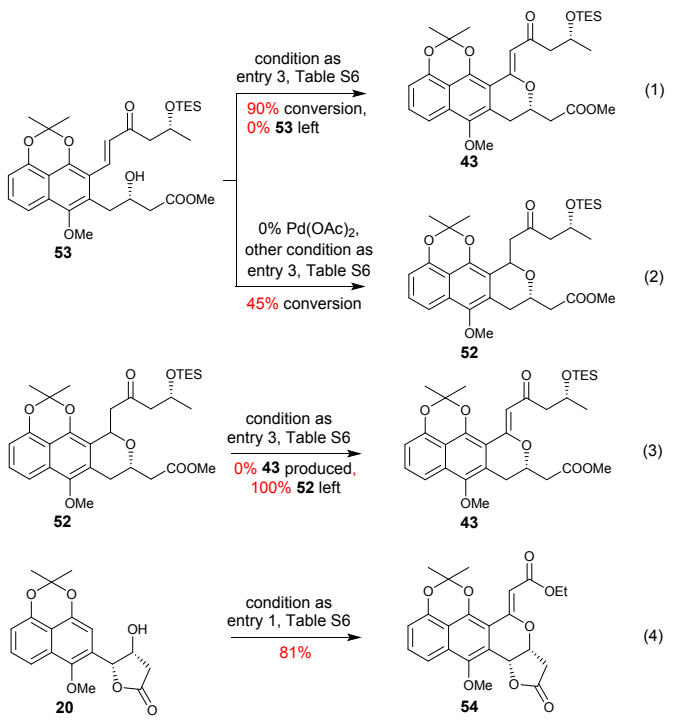

Scheme 4. Reactions relevant to C-H olefination mechanistic considerations.

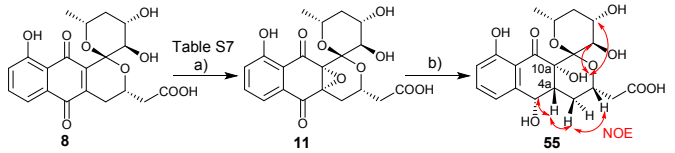

Scheme 5. Synthesis and structural determination of 4a,10a–epoxy-epi-deacetylgriseusin B (11). Key NOE crosspeaks are highlighted (red arrows). Reagents and conditions: (a) H_2O_2, DABCO, DCM, 0 °C-rt, 2 h, 88%; (b) H_2, Pd/C, MeOH, 2 h, 42%.

re-coordination versus nucleophilic attack of the participant hydroxyl (which can be influenced via nucleophile orientation and/or nucleophilicity as noted in Table S6). For example, the higher yield of methylene isochroman **54** is attributed to lower nucleophilicity of the **20**-derived α,β-unsaturated ester (Scheme 4). Cumulatively, these studies provide further support of Yu's[15] and our[3m] previously proposed step-wise mechanism for this oxidative cyclization event.

Guided by our prior success with griseusin A-type spiropyran ring formation, unsaturated ketone **43** was converted to C3'-deshydroxy substrate **44** and C3′-(*S*)-hydroxy substrate **30**, respectively (Scheme 3). The C4′-carbonyl of intermediate **30** was subsequently stereoselectively reduced to obtain **45** followed by hydrolysis with LiOH to give intermediate **46**. In parallel, **30** C3′-*O*-benzyl protection under a mild conditions gave intermediate **47**. Subsequent diastereoselective **47** C4′-ketone reduction with either borane or borohydride gave 4'-(*S*)-alcohol **48** or 4′-*R*-alcohol **50**, respectively. Final standard protecting group manipulations gave key subclass B intermediates **49** and **51**.

2.4 Completion of total syntheses.

The synthesis of *ent*-precursors mirrored that conducted for the preparation of griseusin A/C and B subclasses. For example, *ent*-**45** employed *R*-S_p-josiphos as a chiral catalyst in the enantioselective β-borylation of **27** and α,β-unsaturated ketone handle **29*S*** in the C-H olefination step, while AD-mix-α and ketone **22*S*** were applied to construct *ent*-griseusin C and D scaffolds. With all key griseusin and *ent*-griseusin precursors in hand, final deprotection was accomplished with silver oxide under acidic conditions as summarized in Table 1. Following previously reported oxidative strategies,[16] hydrogen peroxide and DABCO furnished the desired **11** C-4a/C-10a epoxide with 8:1 diastereoselectivity (Scheme 5 and Table S7). In summary, starting from 1,5-dihydroxynaphthalene the divergent strategy put forth enabled access to eleven naturally-occurring griseusins and seven new griseusin analogues in 10-18 steps with total yields ranging from 3-8%.

2.5 Configuration assignment of griseusin B epoxide (11).

While the spectroscopic data for synthetic **11** and previously-isolated **11** were consistent (Table S8), the reported epoxide **11** isolated from *Nocardiopsis* sp. YIM80133 lacked assignment of absolute stereochemistry.[4g] To address this, NMR studies of tetrol **55**, produced via hydrogenation of **11**, enabled assignment of the epoxide absolute stereochemistry as C-4a*R*, 10a*S* (Scheme 5). As biosynthetic transformations are commonly conserved within a given natural product classes, this definitive stereochemical assignment may also be relevant to other naturally-occurring C-4a/C-10a-epoxy PNQs.[1a, 1c, 1m]

2.6 Structural revision of griseusin D (12).

Methanolysis of **18** afforded E-ring lactone **12** in good yield (Scheme 6). While the spectroscopic data for compound **12** was in strong agreement with the reported griseusin D (Table S9),[6f] the determined optical rotation of **12** was diametrically opposed to that reported for griseusin D. Thus, we postulate **12** to be *ent*-griseusin D and the structure of reported griseusin D to be that illustrated in Scheme 6. Consistent with this, most griseusins previously reported from the griseusin D-producing strain (*Nocardiopsis* sp. YIM80133) also displayed negative optical rotations.[6g]

2.7 Griseusin comparative cancer cell line cytotoxicity.

All compounds were tested against four cancer cell lines (non-small cell lung A549, prostate PC3 and colorectal HCT116 and DLD-1) (Table 2). While most griseusins were found to be cytotoxic across this panel, A549 was generally (2- to 10-fold) less susceptible to PNQs. An intact D-lactone ring (*e.g.*, as found in griseusins A and C, compounds **1-4**) was generally advantageous as compared to D-ring open comparators (*e.g.*, griseusins B and D, compounds **6-8, 12**). Surprisingly, active enantiomeric comparators (*e.g.*, **1** vs **5** or **7** vs **9**) displayed similar potencies. E-ring C3'-substitution generally had a negative impact potency (*e.g.*, **2** vs **16**, **3** vs **13**, or **4** vs **17**), while bioactivity was less impacted by C4'-alterations (ketone, *S*-hydroxyl, *R*-hydroxyl). Destruction of the naphthoquinone core also abolished activity (*e.g.*, compounds **11** and **55**).

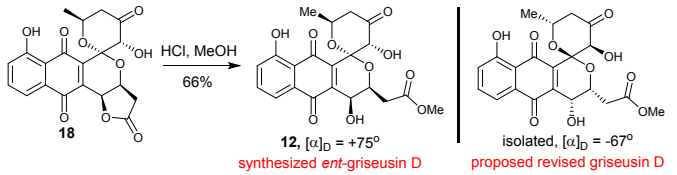

Scheme 6. Synthesis of *ent*-griseusin D (12) and proposed griseusin D structural revision.

Table 1. Total synthesis of natural-occurring griseusins (1-10) and their analogs (13-19).[a]

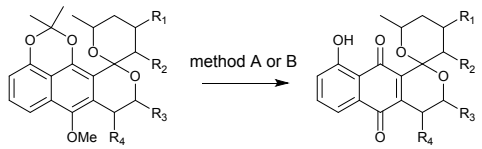

entry	reactant (method [b])	product (yield[c])	entry	reactant (method [b])	product (yield[c])
1	**39** (A)	**1** (81%)	10	*ent*-**46** (A)	**10** (79%)
2	**35** (A)	**2** (85%)	11	**32** (A)	**13** (73%)
3	**23** (A)	**3** (63%)	12	1,3'-*epi*-**23**[f], (A)	**14** (63%)
4	**36** (A)	**4** (62%)	13	**40** (A)	**15** (75%)
5	*ent*-**35** (A)	**5** (77%)	14	**33** (A)	**16** (78%)
6	**51** (B)	**6** (54%[d])	15	**34** (A)	**17** (75%)
7	**46** (B)	**7** (68%)	16	**25** (A)	**18** (63%)
8	**49** (B)	**8** (56% [e])	17	**44** (B)	**19** (52% [d])
9	*ent*-**45** (B)	**9** (55% [e])			

[a]See SI for experimental details. [b]Method A: 5 eq. AgO, 10 eq. 6N HNO_3 at 0 °C for 10 min; method B: 2.2 eq. AgO, 6 eq. 3N HNO_3 at -10 °C for 30 min. [c]Isolated yields. [d]Deprotection of **51** benzyl ether (hydrogenolysis) was conducted before the deprotection step and reported yield included this conversion. [e]Ester hydrolysis of **49** and *ent*-**45** were conducted before the deprotection step and the reported yield included this conversion. [f]See ref 3m for structural detail.

2.8 Griseusins inhibit peroxiredoxin 1 (Prx1) and glutaredoxin 3 (Grx3) and thereby influence 4E-BP1 phosphorylation.

We recently identified the PNQ **FB** as a potent inhibitor of peroxiredoxin 1 (Prx1) and glutaredoxin 3 (Grx3) and determined **FB**'s antitumor effect to be mediated by inhibition of phosphorylation of 4E-BP1.[5] While 4E-BP1 is a cap-dependent translation repressor of oncogenic mRNA translation and tumorigenesis, phosphorylation of 4E-BP1 by mTORC1 relieves its inhibitory control leading to tumor progression.[17] To assess whether griseusin-type PNQs can also bind Prx1 and/or Grx3, we conducted a simple competition assay with model griseusin **13** using the **FB**-based biotinylated probe set from our previously-reported target identification study (Figure 2a).[5] In this study (Figure 2b), **13** could completely block the binding of the active **FB**-based **Probe 1** to Prx1 or Grx3 in HCT116 crude extracts. Consistent with this, **13** also directly inhibited Prx1 and Prx2 catalytic activity with apparent IC_{50}s of 2.3 μM and 7.3 μM, respectively (Figure S1). Similar to the inhibitory effect of **FB** on 4E-BP1 phosphorylation, the representative cytotoxic griseusins tested (*e.g.*, **3**, **13**, **17**, and **19**) inhibited 4E-BP1 phosphorylation while non-cytotoxic analogues (*e.g.*, **11**) had no effect on 4E-BP1p (Figure 2c). Collectively, these findings suggest that griseusin-type and **FB**-type PNQs exhibit a similar mechanism of action.

Table 2. Cancer cell cytotoxicity and inhibition of axolotl tail regeneration.[a]

Cmpd	A549[b]	PC3[b]	HCT116[b]	DLD-1[b]	axolotl tail[c]
1	1.0±0.2	0.1±0.08	0.2±0.08	0.1±0.02	+
2	3.4±1.2	0.9±0.3	0.5±0.1	0.1±0.08	+
3	1.8±0.03	0.1±0.1	0.1±0.02	0.1±0.004	+
4	10.3±7.9	1.9±0.3	>2	>2	-
5	6.9±0.1	0.6±0.02	0.2±0.01	0.2±0.06	N.D.
6	4.1±1.0	2.1±0.9	1.2±0.9	0.6±0.3	+
7	11.6±9.0	0.9±0.5	>2	0.3±0.1	-
8	>20	2.9±0.6	1.2±0.6	>2	-
9	15.1±0.2	0.9±0.08	0.4±0.05	0.3±0.01	-
10	5.0±0.1	0.7±0.01	0.8±0.5	0.5±0.4	toxic
11	>20	>20	>2	>2	-
12	3.2±0.6	1.0±0.3	>2	0.1+0.02	+
13	0.7±0.3	0.1±0.02	0.1±0.06	0.1±0.03	toxic
14	2.1±0.1	1.1±0.3	0.7±0.01	0.9±0.4	-
15	1.2±0.3	0.2±0.06	0.2±0.02	0.1±0.01	+
16	1.0±0.2	0.2±0.1	0.1±0.04	0.1±0.01	toxic
17	1.2±0.2	0.2±0.04	0.1±0.01	0.04±0.01	+
18	2.7±0.5	0.6±0.3	0.2±0.03	0.1±0.03	+
19	1.2±0.2	0.3±0.05	0.1±0.05	0.1±0.06	toxic
55	>20	>20	>2	>2	N.D.

[a]See SI for experimental details. [b]IC_{50}±SD values (μM) from experiments performed in triplicate. The highest concentrations tested were 20 μM (A549 and PC3) and 2 μM (HCT116 and DLD-1), respectively. [c]Results from single dose (10 μM) experiments performed in triplicate where '+' indicates complete inhibition, '-' reflects no effect and 'toxic' denotes lethality.

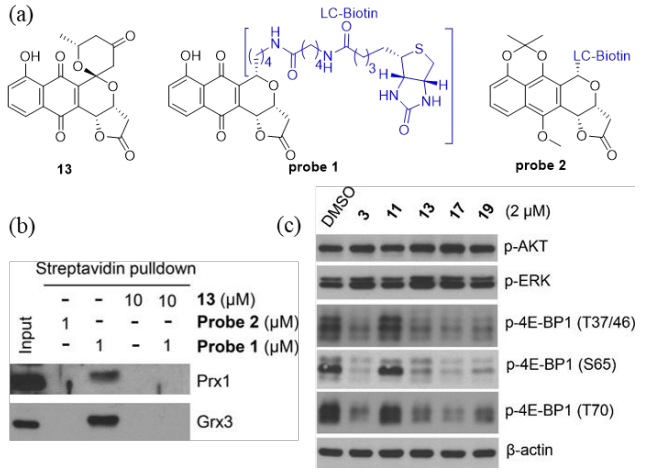

Figure 2. (a) Structures of compound **13** and **probes 1** and **2**. **Probe 1** is active (both cytotoxic and as an inhibitor of 4E-BP1 phosphorylation) while the control **Probe 2** is an inactive comparator. (b) Compound **13** competes with **Probe 1** binding to Prx1 and Grx3. (c) Cytotoxic griseusin-type PNQs effectively inhibit phosphorylation of 4E-BP1 but not AKT and ERK kinases.

2.9 Impact of griseusins on axolotl tail regeneration.

Recent studies in a highly regenerative salamander model (the Mexican axolotl, *Ambystoma mexicanum*) revealed that ROS rapidly increased in response to axolotl tail amputation and was required for tail regeneration.[18] These studies also demonstrated pharmacological inhibition of ROS producing enzymes with diphenyleneiodonium chloride (DPI) and VAS2870 reduced ROS and led to inhibition of cellular proliferation and tail

outgrowth inhibition. To investigate the impact of the Prx1/Grx3-inhibiting griseusins within this context, representative griseusin analogues were evaluated in the same axolotl embryo tail regeneration (ETR) assay.[7] Tail-amputated axolotl embryos were incubated in microtiter plates in the absence (vehicle control, DMSO) or presence of 10 μM agent (**1-4**, **6-19**) and imaged on day 1 (pre-treatment) and day 7. The initial single dose screen revealed a moderate correlation between cancer cell line cytotoxicity and inhibition of tail regeneration (Table 2, Figure S2) where divergence may result, in part, from yet to be determined factors that contribute to differences in uptake and/or in vivo exposure. Importantly, these single dose studies, in conjunction with the subsequent established dose response of both inhibition of tail regeneration and lethality with representative **13** (Figure S3), are consistent with a mechanistic relationship between Prx1/Grx3, ROS and tail regeneration and provide preliminary evidence for in vivo application of griseusin-based probes.

Conclusions

This comprehensive study highlights the first concise and divergent synthetic approach to prepare griseusin A-E analogs. The enabling chemistry put forth facilitated a broad comparative cancer cell line cytotoxicity SAR analysis and in-depth mechanistic studies that established griseusins as inhibitors of Prx1/Grx3 and 4E-BP1 phosphorylation. Importantly, Prx1 and Grx3 overexpression is a hallmark of a variety of cancers and is associated with redox adaptation that promotes tumor progression and resistance to many anticancer agents and radiation.[19] Consistent with this, knockdown of Prx1 and Grx3 expression in cancer cells leads to an increase in ROS levels, resulting in inhibition of proliferation, survival, invasion, metastasis, and sensitivity to chemotherapy and radiation.[19d,20] These studies also suggest that similar subtle shifts in the balance of [ROS] within the axolotl tail regeneration model may also contribute to the observed anti-proliferative effects of griseusins in vivo. Cumulatively, the facile access to the griseusins described herein is expected to enable new molecular probe development to advance the study the role of Prx1 and Grx3 in biology and may also serve as a starting point for early anticancer lead development. Given the established mechanistic relationship between griseusins and **FB** (an effective anticoccidial and antimalarial agent),[1a,4] the current study may also prompt similar functional evaluation of griseusins.

Conflicts of interest

The authors declare the following competing financial interest: J.S.T. is a co-founder of Centrose (Madison, WI, USA).

Acknowledgements

This work was supported by National Institutes of Health grants R01 CA203257 (QBS, JST), R24 OD21479 (SRV, JST), T32 DA016176 (YZ), the University of Kentucky College of Pharmacy, the National Center for Advancing Translational Sciences (UL1TR000117 and UL1TR001998), and the Start-up funding of Jiangsu Specially-Appointed Professor and National Natural Science Foundation of China (No. 21877062, YZ). We also thank Prof. Tyler D. McQuade (Florida State University) generously providing McQuade I NHC copper catalyst.

Human colon (HCT116, DLD-1), prostate (PC3) and lung (A549) cancer cell lines were obtained from the American Type CultureCollection (ATCC, Manassas, VA) and cultured as per ATCC recommendations.

Notes and references

1 (a) G. A. Ellestad, M. P. Kunstmann, H. A. Whaley and E. L. Patterson, *J Am Chem Soc*, 1968, **90**, 1325-1332. (b) S. Omura, K. Tsuzuki, Y. Iwai, M. Kishi, S. Watanabe and H. Shimizu, *J Antibiot (Tokyo)*, 1985, **38**, 1447-1448. (c) T. Okabe, K. Nomoto and N. Tanaka, *J Antibiot (Tokyo)*, 1986, **39**, 1-5. (d) T. W. Yu, M. J. Bibb, W. P. Revill and D. A. Hopwood, *J Bacteriol*, 1994, **176**, 2627-2634. (e) R. J. Cox, T. S. Hitchman, K. J. Byrom, I. S. Findlow, J. A. Tanner, J. Crosby and T. J. Simpson, *FEBS Lett*, 1997, **405**, 267-272. (f) R. J. Zawada and C. Khosla, *J Biol Chem*, 1997, **272**, 16184-16188. (g) J. Crosby, K. J. Byrom, T. S. Hitchman, R. J. Cox, M. P. Crump, I. S. Findlow, M. J. Bibb and T. J. Simpson, *FEBS Lett*, 1998, **433**, 132-138. (h) R. E. Armer, C. J. Dutton, B. R. Fenner, S. D. Greenwood, K. T. Hall and A. J. Rudge, *Bioorg Med Chem Lett*, 1998, **8**, 139-142. (i) R. J. Zawada and C. Khosla, *Chem Biol*, 1999, **6**, 607-615.(j) T. Taguchi, S. Okamoto, K. Hasegawa and K. Ichinose, *Chembiochem*, 2011, **12**, 2767-2773. (k) X. Wang, K. A. Shaaban, S. I. Elshahawi, L. V. Ponomareva, M. Sunkara, Y. Zhang, G. C. Copley, J. C. Hower, A. J. Morris, M. K. Kharel and J. S. Thorson, *J Nat Prod*, 2013, **76**, 1441-1447. (l) X. Wang, S. I. Elshahawi, K. A. Shaaban, L. Fang, L. V. Ponomareva, Y. Zhang, G. C. Copley, J. C. Hower, C. G. Zhan, M. K. Kharel and J. S. Thorson, *Org Lett*, 2014, **16**, 456-459.

2 For the synthetic literatures of various PNQ: (a) M. A. Brimble, L. J. Duncalf and M. R. Nairn, *Nat Prod Rep*, 1999, **16**, 267-281. (b) M. A. Brimble, *Pure Appl. Chem,* 2000, **72**, 1635-1639. (c) J. Sperry, P. Bachu and M. A. Brimble, *Nat Prod Rep*, 2008, **25**, 376-400. (d) J. Jacobs, S. Claessens, K. Huygen, K. A. Tehrani, N. De Kimpe, *Pure Appl. Chem,* 2011, **83**, 1651-1674. (e) B. J. Naysmith, P. A. Hume, J. Sperry and M. A. Brimble, *Nat Prod Rep*, 2017, **34**, 25-61. (f) Y. Zhang, X. Wang, M. Sunkara, Q. Ye, L. V. Ponomereva, Q. B. She, A. J. Morris and J. S. Thorson, *Org Lett*, 2013, **15**, 5566-5569.

3 For the literatures focused on the synthesis of griseusins and their intermediates: (a) T. Kometani, Y. Takeuchi, E. Yoshii, *J. Org. Chem,* 1982, **47**, 4725-4730. (b) T. Kometani, Y. Takeuchi, E. Yoshii, *J. Org. Chem,* 1983, **48**, 2311-2314. (c) N. Tsuji, T. Kamigauchi, H. Nakai, M. Shiro, *Tetrahedron Lett,* 1983, **24**, 389-390. (d) M. A. Brimble, M. R. Nairn, *J. Chem. Soc. Perkin Tran. 1,* 1990, **1**, 169-171. (e) M. A. Brimble, M. R. Nairn, *J. Chem. Soc. Perkin Tran. 1,* 1992, **5**, 579-583. (f) M. A. Brimble, M. R. Nairn, Molecules, 1996**, 1**, 3-14. (g) M. A. Brimble, M. R. Nairn, J. Park, *J. Org. Lett,* 1999, **1**, 1459-1462. (h) M. A. Brimble, M. R. Nairn, J. Park, *J. Chem. Soc. Perkin Trans,* 2000, **5**, 697-709. (i) K. A. Parker, T. L. Mindt and Y. H. Koh, *Org Lett*, 2006, **8**, 1759-1762. (j) B. J. Naysmith and M. A. Brimble, *Org Lett*, 2013, **15**, 2006-2009. (k) B. J. Naysmith, D. Furkert, M. A. Brimble, *Tetrahedron*, 2014, **70**, 1199-1206. (l) X. Jiang, M. Wang, S. Song, Y. Xu, Z. Miao, A. Zhang, *RSC Adv,* 2015, ***5***,

27502-27508. (m) Y. Zhang, Q. Ye, X. Wang, Q. B. She and J. S. Thorson, *Angew Chem Int Ed Engl*, 2015, **54**, 11219-11222.
4 J. T. Fitzgerald, P. P. Henrich, C. O'Brien, M. Krause, E. H. Ekland, C. Mattheis, J. M. Sa, D. Fidock and C. Khosla, *J Antibiot (Tokyo)*, 2011, **64**, 799-801.
5 Q. Ye, Y. Zhang, Y. Cao, X. Wang, Y. Guo, J. Chen, J. Horn, L. V. Ponomareva, L. Chaiswing, K. A. Shaaban, Q. Wei, B. D. Anderson, D. K. St Clair, H. Zhu, M. Leggas, J. S. Thorson and Q. B. She, *Cell Chem Biol*, 2019, **26**, 366-377 e312.
6 For the naturally-occurring griseusin structures: (a) N. Tsuji, M. Kobayashi, Y. Wakisaka, Y. Kawamura and M. Mayama, *J Antibiot (Tokyo)*, 1976, **29**, 7-9. (b) N. Tsuji, M. Kobayashi, Y. Terui, K. Tori, *Tetrahedron*, 1976, **32**, 2207-2210. (c) M. Maruyama, C. Nishida, Y. Takahashi, H. Naganawa, M. Hamada and T. Takeuchi, *J Antibiot (Tokyo)*, 1994, **47**, 952-954. (d) M. Igarashi, W. Chen, T. Tsuchida, M. Umekita, T. Sawa, H. Naganawa, M. Hamada and T. Takeuchi, *J Antibiot (Tokyo)*, 1995, **48**, 1502-1505. (e) X. Li, Y. Zheng, I. Sattler and W. Lin, *Arch Pharm Res*, 2006, **29**, 942-945. (f) Y. Q. Li, M. G. Li, W. Li, J. Y. Zhao, Z. G. Ding, X. L. Cui and M. L. Wen, *J Antibiot (Tokyo)*, 2007, **60**, 757-761. (g) J. He, E. Roemer, C. Lange, X. Huang, A. Maier, G. Kelter, Y. Jiang, L. H. Xu, K. D. Menzel, S. Grabley, H. H. Fiebig, C. L. Jiang and I. Sattler, *J Med Chem*, 2007, **50**, 5168-5175.
7 (a) X. Wang, Y. Zhang, L. V. Ponomareva, Q. Qiu, R. Woodcock, S. I. Elshahawi, X. Chen, Z. Zhou, B. E. Hatcher, J. C. Hower, C. G. Zhan, S. Parkin, M. K. Kharel, S. R. Voss, K. A. Shaaban and J. S. Thorson, *Angew Chem Int Ed Engl*, 2017, **56**, 2994-2998. (b) L. V. Ponomareva, A. Athippozhy, J. S. Thorson and S. R. Voss, *Comp Biochem Physiol C Toxicol Pharmacol*, 2015, **178**, 128-135.
8 Conditions required to remove other potential naphthyl moiety protecting groups (*e.g.*, trimethyl or triacetyl) were anticipated to contribute to C1 epimerization and/or scaffold decomposition.
9 H. C. Kolb, M. S. VanNieuwenhze, K. B. Sharpless, *Chem. Rev,* 1994, **94**, 2483-2547.
10 J. E. Lee and J. Yun, *Angew Chem Int Ed Engl*, 2008, **47**, 145-147.
11 S. Sato, T. Sakamoto, E. Miyazawa, Y. Kikugawa, *Tetrahedron*, 2004, **60**, 7899-7906.
12 (a) J. W. Bosco and A. K. Saikia, *Chem Commun (Camb)*, 2004, DOI: 10.1039/b401218f, 1116-1117. (b) R. Singh, R. M. Kissling, M. A. Letellier and S. P. Nolan, *J Org Chem*, 2004, **69**, 209-212.
13 L. Chiummiento, M. Funicello, P. Lupattelli and F. Tramutola, *Org Lett*, 2012, **14**, 3928-3931.
14 (a) T. Shiomi, T. Adachi, K. Toribatake, L. Zhou and H. Nishiyama, *Chem Commun (Camb)*, 2009, DOI: 10.1039/b915759j, 5987-5989. (b) J. K. Park, H. H. Lackey, M. D. Rexford, K. Kovnir, M. Shatruk and D. T. McQuade, *Org Lett*, 2010, **12**, 5008-5011.
15 Y. Lu, D. H. Wang, K. M. Engle and J. Q. Yu, *J Am Chem Soc*, 2010, **132**, 5916-5921.
16 (a) D. A. Henderson, P. N. Collier, G. Pave, P. Rzepa, A. J. White, J. N. Burrows and A. G. Barrett, *J Org Chem*, 2006, **71**, 2434-2444. (b) K. Tatsuta, Y. Suzuki, T. Toriumi, Y. Furuya, S. Hosokawa, *Tetrahedron Lett,* 2007, **48**, 8018-8021.
17 (a) A. C. Hsieh, Y. Liu, M. P. Edlind, N. T. Ingolia, M. R. Janes, A. Sher, E. Y. Shi, C. R. Stumpf, C. Christensen, M. J. Bonham, S. Wang, P. Ren, M. Martin, K. Jessen, M. E. Feldman, J. S. Weissman, K. M. Shokat, C. Rommel and D. Ruggero, *Nature*, 2012, **485**, 55-61. (b) Q. Ye, W. Cai, Y. Zheng, B. M. Evers and Q. B. She, *Oncogene*, 2014, **33**, 1828-1839. (c) J. Wang, Q. Ye, Y. Cao, Y. Guo, X. Huang, W. Mi, S. Liu, C. Wang, H. S. Yang, B. P. Zhou, B. M. Evers and Q. B. She, *Nat Commun*, 2017, **8**, 2207.
18 N. W. Al Haj Baddar, A. Chithrala and S. R. Voss, *Dev Dyn*, 2019, **248**, 189-196.
19 (a) M.K. Cha and I.H. Kim, *Cancer Epidemiol,* 2009, **33**, 281–287. (b) K. Iwao-Koizumi, R. Matoba, N. Ueno, S. J. Kim, A. Ando, Y. Miyoshi, E. Maeda, S. Noguchi and K. Kato, *J Clin Oncol*, 2005, **23**, 422–431. (c) M. H.Park, M. Jo, Y. R. Kim, C. K. Lee and J. T. Hong, *Pharmacol Ther* 2016, **163**, 1–23. (d) Y. Qu, J. Wang, P. S. Ray, H. Guo, J. Huang, M. Shin-Sim, B. A. Bukoye, B. Liu, A. V. Lee, X. Lin, P. Huang, J. W. Martens, A. E. Giuliano, N. Zhang, N. H. Cheng and X. Cui, *J Clin Invest*, 2011, **121**, 212–225. (e) D. Trachootham, J. Alexandre and Huang, *Nat Rev Drug Discov*, 2009, **8**, 579–591. (f) C. M. Woolston, S. J. Storr, I. O. Ellis, D. A. Morgan and S. G. Martin, *Radiother Oncol*, 2011, **100**, 308–313.
20 (a) M. Bajor, A. O. Zych, A. Graczyk-Jarzynka, A. Muchowicz, M. Firczuk, L. Trzeciak, P. Gaj, A. Domagala, M. Siernicka, A. Zagozdzon, P. Siedlecki, M. Kniotek, P. C. O'Leary, J. Golab and R. Zagozdzon, *Br J Cancer* **2018**, *119*, 873–884. (b) M. F. Chen, P. C. Keng, H. Shau, C. T. Wu, Y. C. Hu, S. K. Liao and W. C. Chen, *Int J Radiat Oncol Biol Phys*, 2006, **64**, 581–591. (c) H. Jiang, L. Wu, M. Mishra, H. A. Chawsheen and Q. Wei, *Am J Cancer Res*, 2014, **4**, 445–460. (d) G. Poschmann, M. Grzendowski, A. Stefanski, E. Bruns, H. E. Meyer and K. Stuhler, *Biochim Biophys Acta*, 2015, **1854**, 624–631.

An efficient divergent synthesis of griseusins enabled SAR studies, mechanistic elucidation and evaluation in an axolotl tail regeneration model.

Graphical Abstrac